

PGMO Lecture: Vision, Learning and Optimization

5. Total Variation ++

Thomas Pock

Institute of Computer Graphics and Vision

February 12, 2020

Overview

Total Variation

Total generalized variation

Optical flow estimation

3D reconstruction

The Mumford-Shah functional

Total roto-translational variation

The total variation

- ▶ The total variation has been introduced to image processing in [Rudin, Osher, Fatemi '92], [Chambolle, Lions '97].
- ▶ It is defined for any function $u \in L^1(\Omega)$

$$\text{TV}(u) = \int_{\Omega} |Du| = \sup \left\{ \int_{\Omega} u \operatorname{div} \varphi : \varphi \in \mathcal{C}_c^1(\Omega, \mathbb{R}^d), \|\varphi\|_{2,\infty} \leq 1 \right\}.$$

- ▶ Allows for discontinuities in u .
- ▶ It is a convex lower-semicontinuous function.

Functions with bounded variation

- The space

$$\text{BV}(\Omega) = \left\{ u \in L^1(\Omega) : \int_{\Omega} |Du| < +\infty \right\},$$

of functions with bounded variations equipped with the norm $\|u\|_{\text{BV}} = \|u\|_{L^1} + \int_{\Omega} |Du|$, is a Banach space.

- The function $|\cdot|$ could be any norm and the dual norm is given by

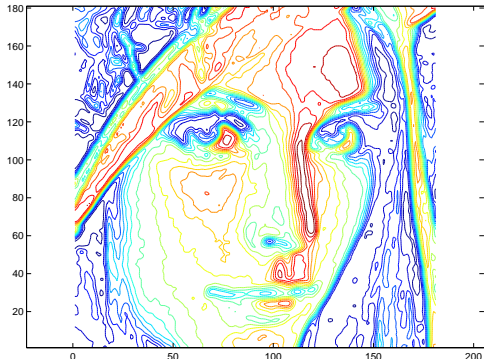
$$|\phi|_* := \sup_{\|x\| \leq 1} \langle \phi, x \rangle$$

- The TV is also well-defined for functions with sharp discontinuities.
- For smooth images, the TV measures the L^1 norm of the image gradient.

$$\text{TV}(u) = \int_{\Omega} |\nabla u| \, dx$$

The coarea formula

- ▶ TV has a nice geometrical interpretation [Fleming and Rishel '60]



- ▶ Can be written in terms of the level sets

$$\int_{\Omega} |Du| = \int_{-\infty}^{\infty} \text{Per} (\{x : u(x) > t\}) dt$$

- ▶ The total variation can be interpreted as the total amount of the level sets perimeters

Shape optimization

- The total variation of a binary function is equivalent to its boundary length. Let $S \subset \Omega$ be a set with smooth boundary, and $u(x) = \mathbf{1}_S(x) = 1$ if $x \in S$ and $\mathbf{1}_S(x) = 0$ else, a binary function associated with the set, then

$$\int_{\Omega} |Du| = \int_{\Omega} |D\mathbf{1}_S| = \text{Per}(S; \Omega),$$

which is exactly the perimeter of the set S .

- This property can be exploited for image segmentation and shape optimization



(a) large TV



(b) medium TV



(c) small TV

Image segmentation

- ▶ Let us assume we have given two functions $p(I|F)$ and $p(I|B)$, which describe the color distributions in a foreground (F) or background (B) region of an image I .
- ▶ The negative log ratio function

$$w(x) = -\log \left(\frac{p(I(x)|F)}{p(I(x)|B)} \right)$$

can be used to determine the likelihood of an image color $I(x)$ to correspond more to the foreground or background region.

- ▶ Consider the following energy

$$\min_{u(x) \in \{0,1\}} \lambda \int_{\Omega} |Du| + \int_{\Omega} u(x) w(x) \, dx$$

- ▶ The model tries to minimize a tradeoff between the boundary length of the binary function u and tries to partition the image into a foreground region $u(x) = 1$ and a background region $u(x) = 0$.

Relation to the ROF model

- ▶ For a pixel x , where $p(I(x)|F) > p(I(x)|B)$ it follows that $w(x) < 0$. The model will have a preference for $u(x) = 1$ (foreground).
- ▶ For a pixel x , with $p(I(x)|F) < p(I(x)|B)$, one has $w(x) > 0$ and hence the model will have a preference for $u(x) = 0$ (background).
- ▶ There is a very interesting relation between the image segmentation model and the ROF model
- ▶ The solution of the image segmentation model is given by

$$u^*(x) = \mathbf{1}_{\{v^* \leq 0\}}(x),$$

where v^* is the minimizer of the ROF model [Chambolle '05], [Berkels '09]

$$\min_v \int_{\Omega} |Dv| + \frac{\lambda}{2} \|v - w\|^2$$

- ▶ Hence, the solution is given by "denoising" the weight function w and thresholding the result at 0.

tv-seg.ipynb

Example



(a) Input image



(b) Weight function



(c) Segmentation



(d) Background removal

Inpainting

- ▶ The total variation can also be used for image inpainting
- ▶ Assume, we have given an image f but only at some locations $D \subset \Omega$ of the image domain

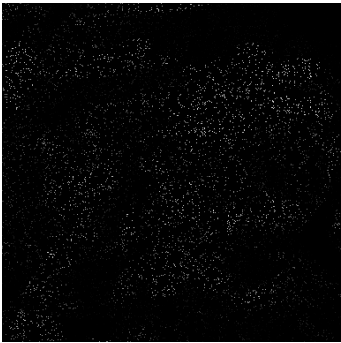
$$\min_u \int_{\Omega} |Du| \quad \text{subject to: } u(x) = f(x) \quad \forall x \in D$$

- ▶ The model tries to reconstruct an image u that coincides with f at the given locations and has a low total variation

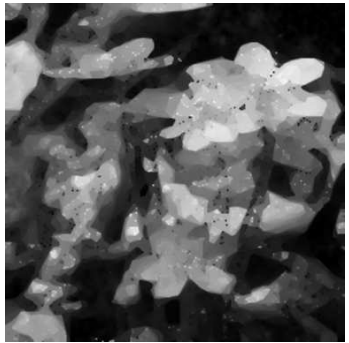
Example



(a) Original image

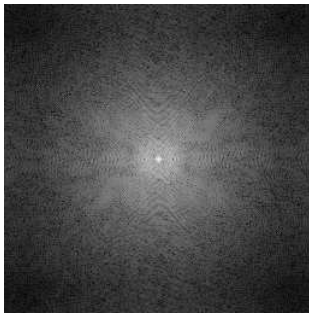


(b) 95% lost pixels



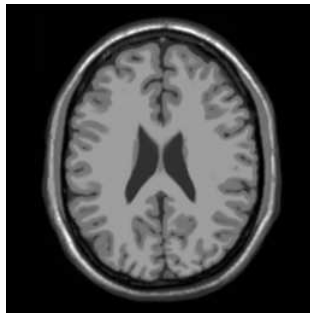
(c) TV

MRI reconstruction in a nutshell

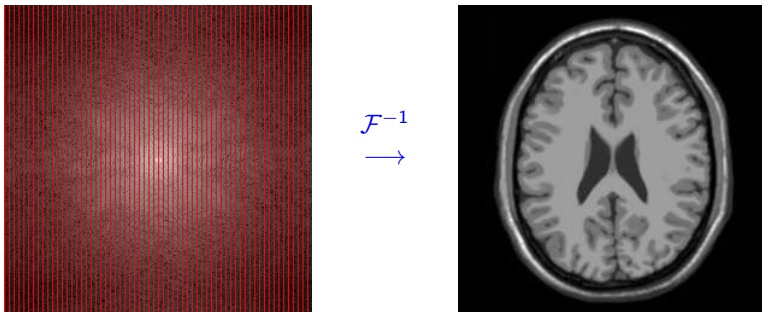


$$\mathcal{F}^{-1}$$

→



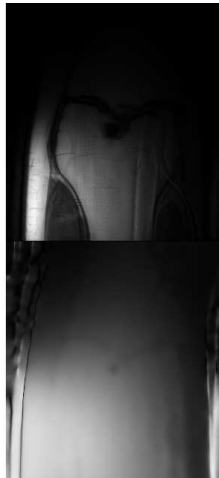
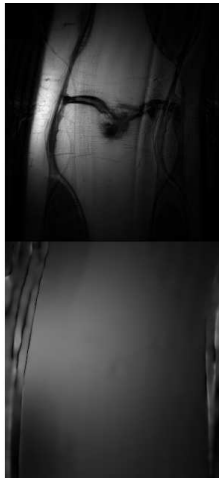
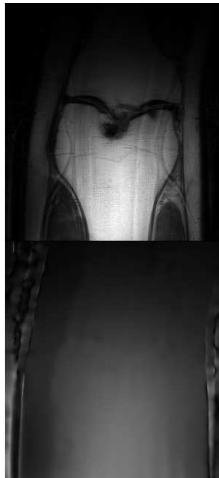
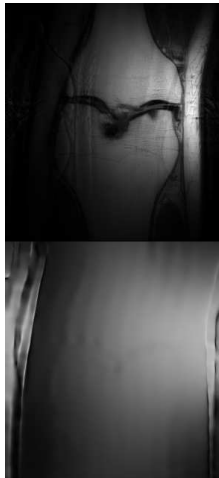
MRI reconstruction in a nutshell



- ▶ Hydrogen nuclei emit a detectable radio frequency signal after applying a high-frequency pulse
- ▶ Receiver coil acquires a line in the Fourier domain (k-space)
- ▶ Wait some time due to physical limits
- ▶ Scantime: 256x256 image $\approx 4\text{min}$

Parallel MRI in a nutshell

- ▶ Combine data from **multiple** receiver coils
- ▶ Each coil is sensitive only in a certain spatial region
- ▶ Used for accelerated MRI



Linear reconstruction (SENSE)

Physically motivated data term: [Pruessmann '99]

$$\frac{1}{2} \|Au - f\|_2^2,$$

where u is the reconstructed image, f holds the measured (sparse) k-space data, and A is a linear operator such that

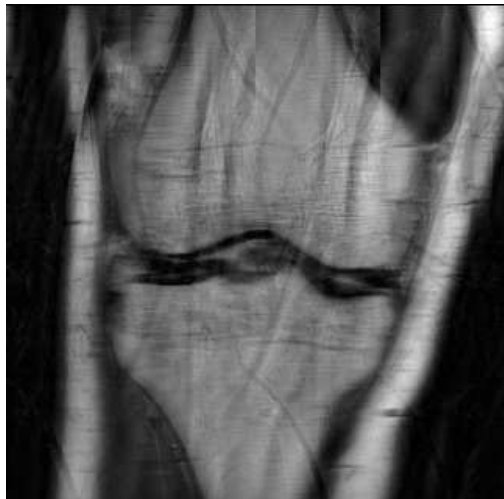
$$Au = S \begin{pmatrix} \mathcal{F}(c_1 \cdot u) \\ \vdots \\ \mathcal{F}(c_Q \cdot u) \end{pmatrix},$$

where \mathcal{F} denotes the Fourier transform, c_1, \dots, c_Q are the sensitivities of the receiver coils and S is a sampling operator.

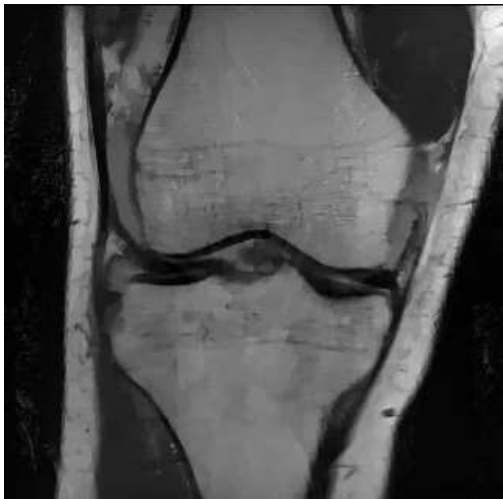
Total Variation based reconstruction

$$\min_u \lambda \int_{\Omega} |Du| + \frac{1}{2} \|Au - f\|_2^2.$$

Example: MRI knee



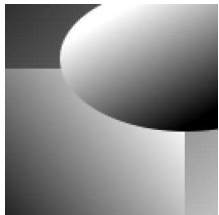
(d) No regularization



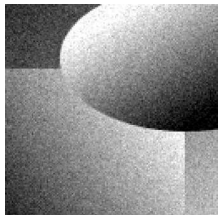
(e) TV regularization

Shortcomings of the total variation

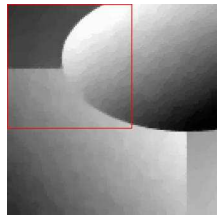
- **Staircasing effect:** The total variation tends to favor piecewise constant solutions



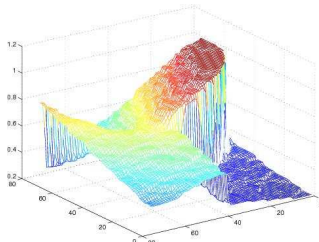
(a) Original



(b) Noisy



(c) ROF



(d) Graph of u

Huber-TV

- A simple idea to reduce the staircasing effect is to replace the 2-norm $|x|$ by a Huber-function $|x|_\varepsilon$ defined by

$$|x|_\varepsilon = \begin{cases} \frac{|x|^2}{2\varepsilon} + \frac{\varepsilon}{2} & \text{if } |x| \leq \varepsilon \\ |x| & \text{else} \end{cases}$$



(a) Noisy image



(b) ROF



(c) Huber-ROF

Overview

Total Variation

Total generalized variation

Optical flow estimation

3D reconstruction

The Mumford-Shah functional

Total roto-translational variation

Total generalized variation

- ▶ There have been several attempts to generalize the total variation to higher order smoothness
- ▶ One example is via infimal convolution [Chambolle, Lions '97]

$$IC(u) = \min_{u=u_1+u_2} \int_{\Omega} |Du_1| + \int_{\Omega} |D^2u_2|$$

- ▶ Another variant, called total generalized variation (TGV) has been proposed in [Bredies, Kunisch, P. '10]

$$\begin{aligned} TGV_{\lambda}^k(u) &= \sup \left\{ \int_{\Omega} u(x) \operatorname{div}^k \varphi(x) dx : \right. \\ &\quad \left. \varphi \in C_c^k(\Omega; \operatorname{Sym}^k(\mathbb{R}^d)), \left\| \operatorname{div}^l \varphi(x) \right\|_{\infty} \leq \lambda_l, l = 0 \dots k-1 \right\} \end{aligned}$$

- ▶ For $k = 2$ and in 1D, both variants are the same

Second order TGV

- ▶ In case, $k = 2$ one can give a more intuitive formulation of TGV

$$\text{TGV}_\lambda^2(u) = \inf_v \lambda_1 \int_{\Omega} |Du - v| + \lambda_0 \int_{\Omega} |Dv|,$$

where $u \in BV(\Omega)$ and $v \in BV(\Omega; \mathbb{R}^2)$

- ▶ This gets rid of the staircasing effect on affine parts of the image
- ▶ We introduce the discrete scalar images $u, f \in \mathbb{R}^{m \times n}$ and vectorial image $\mathbf{v} = (v_1, v_2) \in \mathbb{R}^{m \times n \times 2}$.
- ▶ The discrete (non-symmetric) counterpart of a TGV variant of the ROF model is given by

$$\min_{u,v} \lambda_1 \|Du - \mathbf{v}\|_{2,1} + \lambda_0 \|\mathbf{D}\mathbf{v}\|_{2,1} + \frac{1}{2} \|u - f\|^2,$$

where $\mathbf{D} : \mathbb{R}^{m \times n \times 2} \rightarrow \mathbb{R}^{m \times n \times 4}$ is again a finite differences operator which can be decomposed as $\mathbf{D}\mathbf{v} = (Dv_1, Dv_2)$, where D

Saddle point formulation

- The discrete first- and second-order variations are given by

$$\begin{aligned}\|\mathbf{D}u - \mathbf{v}\|_{2,1} &= \sum_{i=1,j=1}^{m,n} \sqrt{((\mathbf{D}u)_{i,j,1} - v_{i,j,1})^2 + ((\mathbf{D}u)_{i,j,2} - v_{i,j,2})^2}, \\ \|\mathbf{D}\mathbf{v}\|_{2,1} &= \sum_{i=1,j=1}^{m,n} \sqrt{(\mathbf{D}v_1)_{i,j,1}^2 + (\mathbf{D}v_1)_{i,j,2}^2 + (\mathbf{D}v_2)_{i,j,1}^2 + (\mathbf{D}v_2)_{i,j,2}^2}.\end{aligned}$$

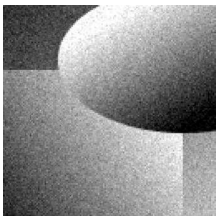
- In order to minimize it, we rewrite it as the saddle-point problem

$$\min_{u,v} \max_{\mathbf{p},\mathbf{q}} \langle \mathbf{D}u - \mathbf{v}, \mathbf{p} \rangle + \langle \mathbf{D}\mathbf{v}, \mathbf{q} \rangle + \frac{1}{2} \|u - f\|^2 - \delta_{\{\|\cdot\|_{2,\infty} \leq \lambda_1\}}(\mathbf{p}) - \delta_{\{\|\cdot\|_{2,\infty} \leq \lambda_0\}}(\mathbf{q}),$$

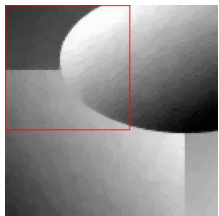
where $\mathbf{p} = (p_1, p_2) \in \mathbb{R}^{m \times n \times 2}$ and $\mathbf{q} = (q_1, q_2, q_3, q_4) \in \mathbb{R}^{m \times n \times 4}$ are the dual variables

tv-vs-tgv2.ipynb

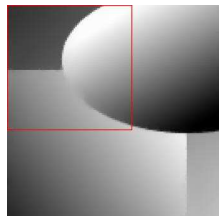
Example



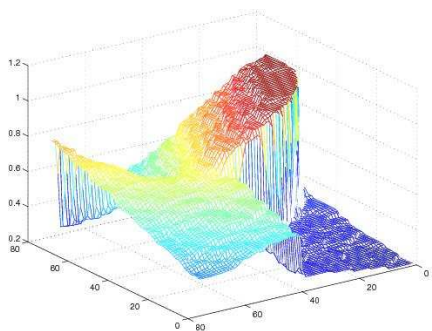
(a) Noisy



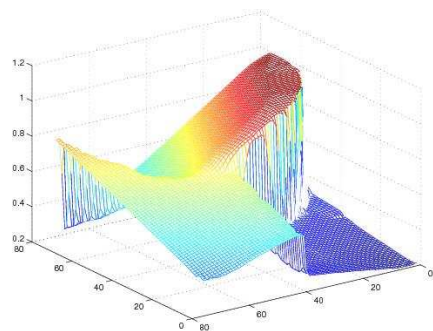
(b) ROF



(c) TGV2



(d) Graph of ROF

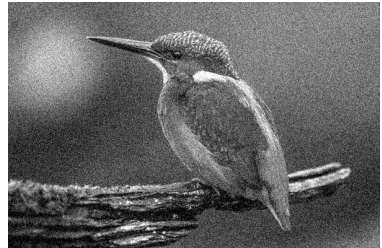


(e) Graph of TGV2

Denoising Example



(a) original image g



(b) noisy image f



(c) ROF, $\lambda = 0.1$



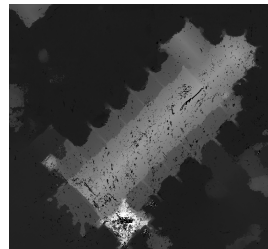
(d) TGV2, $\lambda_{0,1} = (1/4, 1/9)$

TGV-based depth map fusion

- ▶ Assume we have given a number of noisy depth maps $d_i, i = 1, \dots, n$.



...

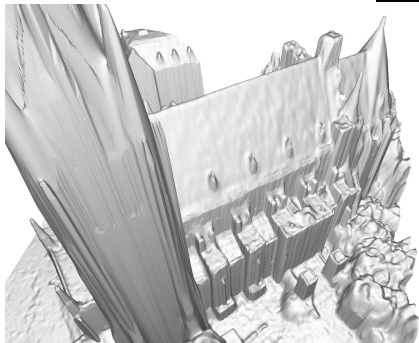
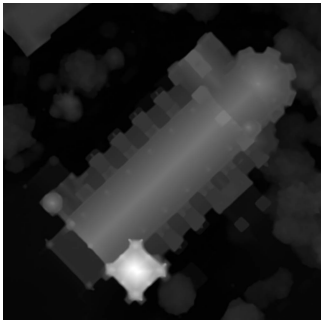


- ▶ The TGV² regularizer can be expected to be a good model for recovering piecewise affine depth maps.
- ▶ We can consider the following TGV based denoising model, that takes into account the multiple depth maps [P., Zebedin, Bischof '11]:

$$\min_u \text{TGV}_\lambda^2(u) + \sum_{i=1}^n \|u - d_i\|_1$$

- ▶ The proximal map to multiple ℓ_1 norm data terms can be computed in closed form using a generalized median formula [Li, Osher '12].

Example



Vectorial total variation

- ▶ So far we have considered only scalar valued images
- ▶ Assume, we have given vector valued images $\mathbf{u} = (u_1, \dots, u_k)$, e.g. RGB images.
- ▶ The question is, what is a good generalization of the total variation to such vector valued images?
- ▶ In principle, we could use any matrix norm acting on the Jacobian $D\mathbf{u}$
- ▶ An interesting class of matrix norms is given by p -Schatten norms

$$\begin{aligned}|J(x)|_{\mathcal{S}_p} &= \left(\sum_{n=1}^{\min\{d,k\}} \sigma_n^p(J(x)) \right)^{\frac{1}{p}}, \quad \forall p \in [1, \infty), \\ |J(x)|_{\mathcal{S}_{\infty}} &= \max_{n \in \{1, \dots, \min\{d, k\}\}} \sigma_n(J(x)),\end{aligned}$$

where the $\sigma_n(J(x))$ denote the singular values of the Jacobian $J(x)$

Vectorial ROF model

- ▶ In case $p = 2$, the Schatten norm corresponds to the Frobenius norm
- ▶ In case $p = 1$, the Schatten norm is equal to the nuclear norm and hence forces the Jacobian to be of low rank [Duran, Möller, Sbert, Cremers '16]
- ▶ In case $p = \infty$, we obtain the operator norm, which penalizes the largest singular value
- ▶ A discrete version of the vectorial ROF model ($p = 1$) is

$$\min_{\mathbf{u}} \lambda \|\mathbf{Du}\|_{\mathcal{S}_1,1} + \frac{1}{2} \|\mathbf{u} - \mathbf{f}\|^2$$

- ▶ The corresponding saddle point formulation is given by

$$\min_{\mathbf{u}} \max_{\mathbf{P}} \langle \mathbf{Du}, \mathbf{P} \rangle + \frac{1}{2} \|\mathbf{u} - \mathbf{f}\|^2 + \delta_{\{\|\cdot\|_{\mathcal{S}_{\infty},\infty} \leq \lambda\}}(\mathbf{P}),$$

- ▶ The projection can be done using a singular value decomposition [Cai, Candés, Shen '10].

Example



(a) original image



(b) noisy image



(c) Frobenius, $\lambda = 0.1$



(d) nuclear, $\lambda = 0.1$

Other analysis operators

- ▶ The gradient operator in TV based models is very simple and does not capture the complicated statistics of natural images
- ▶ In the discrete setting, one can replace the finite differences operator \mathbf{D} by a more general analysis operator
- ▶ Let $\Phi : \mathbb{R}^{m \times n} \rightarrow \mathbb{C}^{k_1 \times \dots \times k_K}$ be a linear transform that maps an image of size $m \times n$ pixels to a complex space of dimension $k_1 \times \dots \times k_K$
- ▶ This includes for example wavelet-like transforms such as the shearlets [Guo, Kutyniok, Labate '06] which provide optimal sparse approximations of cartoon-like images
- ▶ A straight forward extension of the ROF model is given by

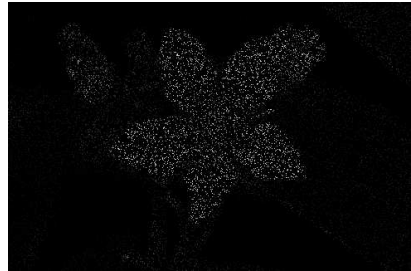
$$\min_u \lambda \|\Phi u\|_1 + \frac{1}{2} \|u - f\|_2^2.$$

- ▶ Can be combined with any reasonable data term, e.g. inpainting

Inpainting



(a) original image



(b) 90% missing data



(c) TV regularization



(d) shearlet regularization

Overview

Total Variation

Total generalized variation

Optical flow estimation

3D reconstruction

The Mumford-Shah functional

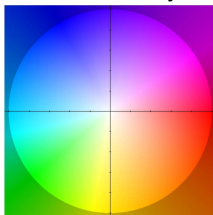
Total roto-translational variation

Optical Flow

- ▶ Optical flow is the *apparent motion* in an image sequence
- ▶ It is a major task of every biological and artificial visual system
- ▶ Can be described by a vector field that transforms one frame in a sequence into the next frame



- ▶ Visualization: Middlebury color code

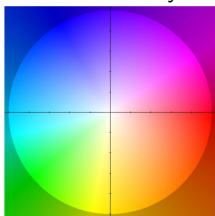


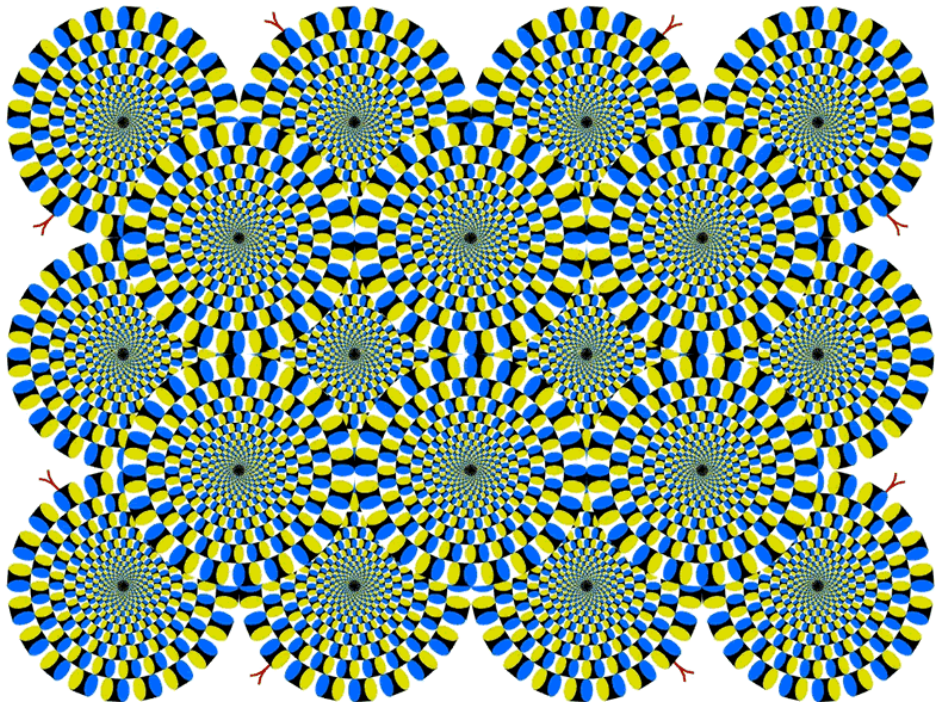
Optical Flow

- ▶ Optical flow is the *apparent motion* in an image sequence
- ▶ It is a major task of every biological and artificial visual system
- ▶ Can be described by a vector field that transforms one frame in a sequence into the next frame



- ▶ Visualization: Middlebury color code



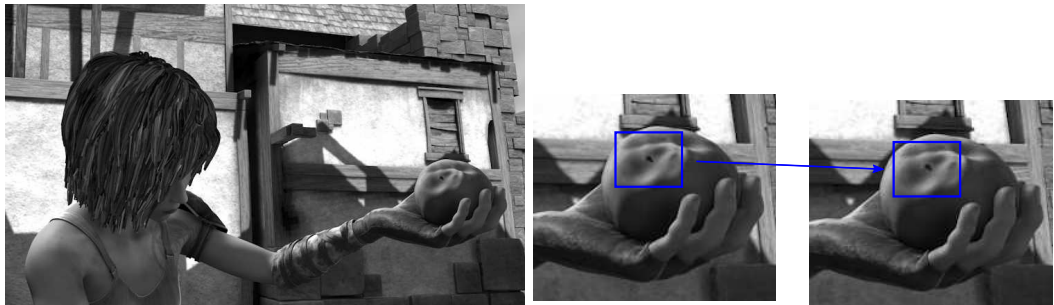


Brightness constancy assumption (BCA)

- ▶ Intensity patterns only change their position

$$I(x, t) \rightarrow I(x + \Delta x, t + \Delta_t)$$

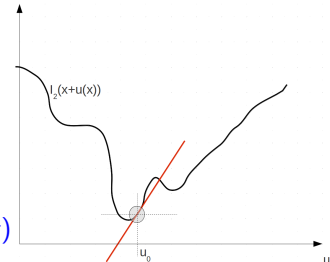
- ▶ $x = \begin{pmatrix} x_1 \\ x_2 \end{pmatrix}$ is a pixel position, $\Delta x = \begin{pmatrix} \Delta x_1 \\ \Delta x_2 \end{pmatrix}$ is the displacement vector



Optical Flow Constraint (OFC)

- ▶ Brightness constancy assumption (BCA)

$$I(x + \Delta_x, t + \Delta_t) = I(x, t)$$



- ▶ Assuming Δ_x, Δ_t are small we can make a first-order Taylor expansion
- ▶ This gives the *optical flow constraint* (or linearized brightness constancy assumption)

$$\nabla_x I(x, t) \cdot u(x) + I_t(x, t) = 0,$$

where $u = (u_1, u_2)^T$ is the velocity vector.

- ▶ To account for larger Δ_x, Δ_t , one makes use of image warping, i.e. by a geometric transformation $\tilde{I}(x, t) = I(x + u^0(x, t), t)$

$$\nabla_x \tilde{I}(x, t) \cdot (u(x) - u^0(x)) + \tilde{I}_t(x, t) = 0,$$

where \tilde{I} is the warped space time intesity function and u^0 is some given velocity field.

TV- ℓ_1 Optical flow

- ▶ Based on the OFC, we can define a variational model to compute the optical flow
- ▶ The most simple one is based on total variation regularization and a ℓ_1 norm penalizing deviations from the OFC

$$\min_{u=(u_1, u_2)} \lambda \operatorname{TV}(u) + \left\| \nabla_x \tilde{I} \cdot (u - u^0) + \tilde{I}_t \right\|_1$$

- ▶ Allows for motion discontinuities and outliers in the OFC (e.g. occlusions)
- ▶ Can be extended to better regularization, e.g. **TGV²**.

Discretizing the OFC

- ▶ In practice, we assume a discrete time and hence we define $I_1(x) = I(x, t)$ and $I_2(x) = I(x, t + \Delta_t)$.
- ▶ Moreover, we use the initial flow field u^0 to “warp” the second image i.e. $\tilde{I}_2(x) = I_2(x + u^0(x, t))$.
- ▶ The time-derivative is approximated via forward differences:

$$\tilde{I}_t(x, t) \approx \frac{\tilde{I}_2(x) - I_1(x)}{\Delta_t}.$$

- ▶ Moreover, our images are spatially discrete and hence the spatial derivatives are usually approximated via

$$\nabla I(x, t) \approx \frac{1}{2} \left(\begin{array}{l} \frac{I_1(x_1 + \Delta_x, x_2) - I_1(x_1 - \Delta_x, x_2)}{2\Delta_x} \\ \frac{I_1(x_1, x_2 + \Delta_x) - I_1(x_1, x_2 - \Delta_x)}{2\Delta_x} \end{array} \right) + \frac{1}{2} \left(\begin{array}{l} \frac{\tilde{I}_2(x_1 + \Delta_x, x_2) - \tilde{I}_2(x_1 - \Delta_x, x_2)}{2\Delta_x} \\ \frac{\tilde{I}_2(x_1, x_2 + \Delta_x) - \tilde{I}_2(x_1, x_2 - \Delta_x)}{2\Delta_x} \end{array} \right).$$

- ▶ Observe that in the above formula, we also average in time, in order that the spatial derivatives “live” at the same time as the time derivative.

Discrete $\text{TV} - \ell_1$ method

- The discrete $\text{TV} - \ell_1$ model is given by

$$\min_{\mathbf{u}} \lambda \|\mathbf{Du}\|_1 + \|\nabla \tilde{I} \cdot (\mathbf{u} - \mathbf{u}^0) + \tilde{I}_t\|_1$$

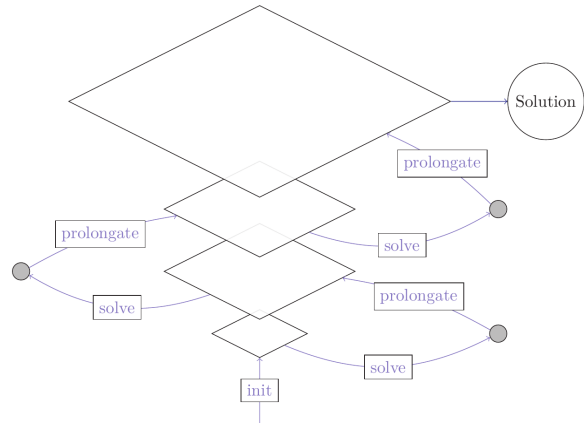
- Can be rewritten as a saddle-point problem and then solved by the primal-dual algorithm.
- The proximal map is given by

$$\text{prox}_{\tau g}(\bar{\mathbf{u}}) = \bar{\mathbf{u}} + \begin{cases} \tau \nabla \tilde{I} & \text{if } \nabla \tilde{I} \cdot (\bar{\mathbf{u}} - \mathbf{u}^0) + \tilde{I}_t < -\tau |\nabla \tilde{I}|^2, \\ -\tau \nabla \tilde{I} & \text{if } \nabla \tilde{I} \cdot (\bar{\mathbf{u}} - \mathbf{u}^0) + \tilde{I}_t > \tau |\nabla \tilde{I}|^2, \\ -\nabla \tilde{I} \cdot (\bar{\mathbf{u}} - \mathbf{u}^0) \frac{\nabla \tilde{I}}{|\nabla \tilde{I}|^2} & \text{if } |\nabla \tilde{I} \cdot (\bar{\mathbf{u}} - \mathbf{u}^0) + \tilde{I}_t| \leq \tau |\nabla \tilde{I}|^2 \end{cases}$$

- Simple pointwise soft-thresholding formula.

Coarse-to-fine framework

- ▶ Compute image pyramids
- ▶ init: initialize flow field
- ▶ solve
 - ▶ warp
 - ▶ linearize
 - ▶ Solve $\text{TV} - \ell_1$
- ▶ prolongate
 - ▶ initialize next level using interpolation and scaling of the flow field



Example



TV- ℓ_1 result



ground truth

Example



TV- ℓ_1 result



ground truth

Realtime optical flow

[Werlberger et al. '11]

Improving optical flow

- ▶ The OFC is based on brightness constancy assumption
- ▶ Changing illumination induces a flow field that does not correspond to the motion of the object



Improving optical flow

- ▶ The OFC is based on brightness constancy assumption
- ▶ Changing illumination induces a flow field that does not correspond to the motion of the object



Improving optical flow

- ▶ Perform structure-texture decomposition
 1. Low-pass filter image (e.g. Gauss or TV denoising)
 2. Subtract low-pass filtered image from original
 3. work with resulting image
- ▶ Although the absolute intensity value changes, the texture part stays the same



(a) Original



(b) Structure part



(c) Texture part

Improving optical flow

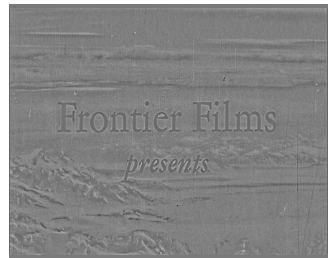
- ▶ Perform structure-texture decomposition
 1. Low-pass filter image (e.g. Gauss or TV denoising)
 2. Subtract low-pass filtered image from original
 3. work with resulting image
- ▶ Although the absolute intensity value changes, the texture part stays the same



(a) Original



(b) Structure part



(c) Texture part

Illumination adaptive $\text{TV} - \ell_1$ optical flow

- ▶ Assuming the illumination changes are additive, we can consider a modified OFC

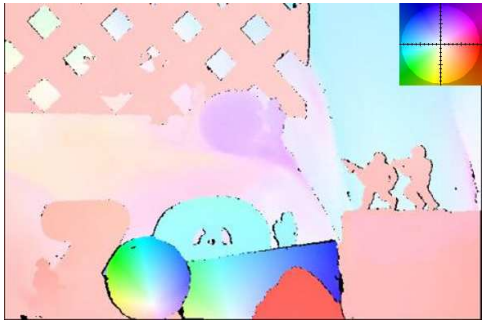
$$\nabla_x \tilde{I}(x, t) \cdot (u(x) - u^0(x)) + \tilde{I}_t(x, t) + \beta v(x, t) = 0,$$

where $\beta > 0$ adjusts the influence of the correction term $v(x, t)$.

- ▶ $v(x, t)$ captures the additive illumination changes, which are assumed to be spatially smooth (e.g. shadows).
- ▶ Hence, we can consider the following illumination adaptive $\text{TV} - \ell_1$ optical flow model

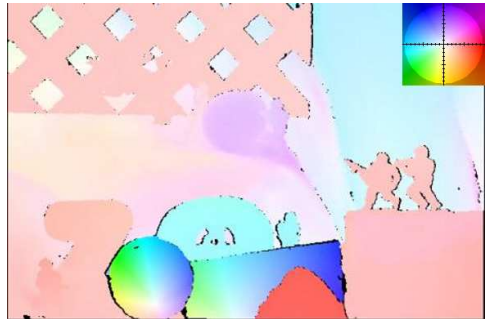
$$\min_{u=(u_1, u_2), v} \lambda \text{TV}(u, v) + \left\| \nabla_x \tilde{I} \cdot (u - u^0) + \tilde{I}_t + \beta v \right\|_1$$

Example



Illumination adaptive $\text{TV} - \ell_1$ result

Example



Illumination adaptive $\text{TV} - \ell_1$ result

Overview

Total Variation

Total generalized variation

Optical flow estimation

3D reconstruction

The Mumford-Shah functional

Total roto-translational variation

Stereo

- ▶ If I_1 and I_2 come from a stereo camera or a moving camera that browses a static scene, the displacement can be restricted to 1D problems on the epipolar lines, [Slesareva, Bruhn, Weickert '05]
- ▶ Each stereo pair can be normalized (rectified) such that the displacement is only one horizontally
- ▶ The depth z can be computed from the displacement u via

$$z(x, y) = \frac{bf}{u(x, y)}$$

where b is the baseline and f is the focal length of the camera

TGV-based stereo for autonomous driving

[Ranftl, Gehrig, P., Bischof '12] (data courtesy of Daimler)

TGV-based stereo for autonomous driving

[Ranftl, Gehrig, P., Bischof '12] (data courtesy of Daimler)

TGV-based stereo for autonomous driving

[Ranftl, Gehrig, P., Bischof '12] (data courtesy of Daimler)

TGV-based stereo for autonomous driving

[Ranftl, Gehrig, P., Bischof '12] (data courtesy of Daimler)

TGV-based shape from focus

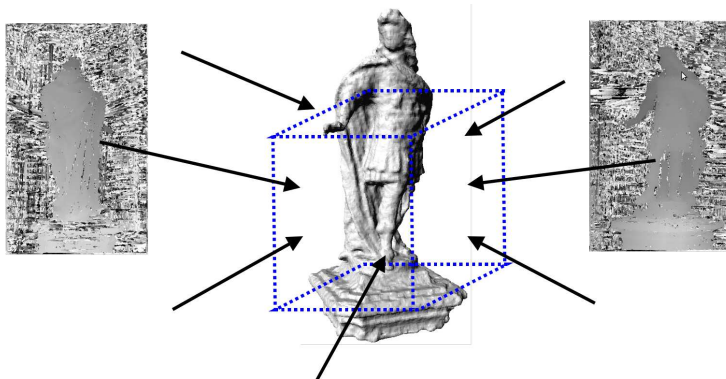


[Heber, P. '13]

Joint work with Alicona Imaging (Graz)

Online 3D reconstruction

- ▶ Volumetric range image integration



- ▶ Surface is represented as the zero level set of a signed distance function

Online 3D reconstruction

- ▶ Volumetric TV- L^1 range integration [Zach, P., Bischof, '07], [Graber, P., Bischof, '11], [Schroers et al. '12]
- ▶ Objective function:

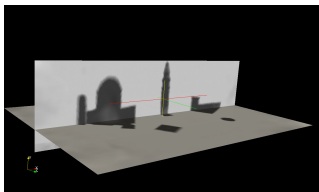
$$\min_u \lambda \operatorname{TV}(u) + \sum_{i=1}^n \|u - f_i\|_1,$$

where f_i are the given 3D distance fields and u is the final, regularized 3D distance function

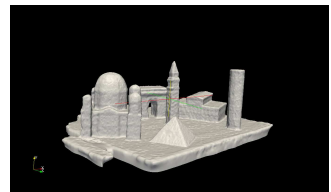
- ▶ Minimizes surface area and ℓ_1 distance to the given distance fields



(a) 3D Scene



(b) Volume



(c) Surface

Overview

Total Variation

Total generalized variation

Optical flow estimation

3D reconstruction

The Mumford-Shah functional

Total roto-translational variation

The Mumford-Shah problem

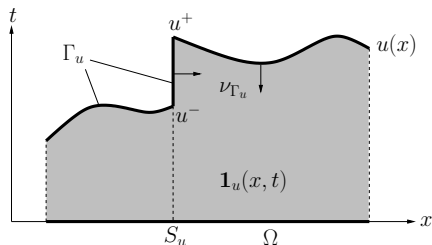
- ▶ Piecewise smooth approximation of functions [Mumford, Shah '89]
- ▶ Variational free boundary problem

$$\min_u MS(u) = \int_{\Omega \setminus S_u} |\nabla u|^2 \, dx + \nu \mathcal{H}^{d-1}(S_u) + \lambda \int_{\Omega} (u - f)^2 \, dx$$

- ▶ Computing a minimizer of the Mumford-Shah functional poses a difficult minimization problem due to its non-convexity
 - ▶ Simulated annealing [Geman, Geman '84]
 - ▶ Graduated non-convexity (GNC) procedure [Blake, Zisserman '87]
 - ▶ Phase field approximation of [Ambrosio, Tortorelli, '90]
 - ▶ Curve evolution via level set methods [Vese, Chan '02]

The approach of Alberti, Bouchitte and Dal Maso

- ▶ The Euler-Lagrange equations of the Mumford-Shah functional provide only a necessary condition for minimality
- ▶ In [Alberti, Bouchitte, Dal Maso, '03], the authors provide a sufficient condition for (some) minimizers of the Mumford-Shah functional.
- ▶ The basic idea is to consider the graph Γ_u of u instead of the function u
- ▶ Rewrite the Mumford-Shah functional by means of the flux of a suitable vector field φ through the graph Γ_u

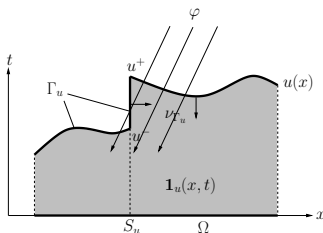


$$\mathbf{1}_u(x, t) = \begin{cases} 1 & \text{if } t < u(x), \\ 0 & \text{else,} \end{cases}$$

A lower bound

- ▶ Suppose, the maximum flux of a vector field $\varphi = (\varphi^x, \varphi^t)$ through the graph provides a lower bound to the Mumford-Shah energy

$$MS(u) \geq \sup_{\varphi \in \mathcal{K}} \int_{\Gamma_u} \varphi \cdot \nu_{\Gamma_u} \, d\mathcal{H}^2.$$



- ▶ It turns out that the above relation is true for

$$\mathcal{K} = \left\{ \varphi \mid \varphi^t(x, t) \geq \frac{\varphi^x(x, t)^2}{4} - \mu(t - f(x))^2, \left| \int_{t_1}^{t_2} \varphi^x(x, s) \, ds \right|_2 \leq \nu \right\}$$

A sufficient condition

- The integral can be extended to $\Omega \times \mathbb{R}$

$$MS(u) = \sup_{\varphi \in \mathcal{K}} \int_{\Omega \times \mathbb{R}} \varphi \cdot D\mathbf{1}_u,$$

- The key observation is now: If for a given u the supremum is attained by a divergence-free vector field $\varphi_u \in \mathcal{K}$, one has

$$MS(v) = \sup_{\varphi \in \mathcal{K}} \int_{\Omega \times \mathbb{R}} \varphi \cdot D\mathbf{1}_v \geq \int_{\Omega \times \mathbb{R}} \varphi_u \cdot D\mathbf{1}_v = \int_{\Omega \times \mathbb{R}} \varphi_u \cdot D\mathbf{1}_u = MS(u),$$

for any v which agrees with u on the boundary of Ω

- Hence u is a minimizer of the Mumford-Shah functional
- If the vector field is divergence-free, it is called a “calibration”
- It remains unclear if a calibration exists for each minimizer ...

Convex relaxation

- ▶ Relaxation of the binary function $\mathbf{1}_u : \Omega \rightarrow \{0, 1\}$ to functions $v : \Omega \rightarrow [0, 1]$
- ▶ Results in the convex-concave saddle-point problem

$$\min_{v \in \mathcal{BV}(\Omega \times \mathbb{R}, [0,1])} \left\{ \sup_{\varphi \in \mathcal{K}} \int_{\Omega \times \mathbb{R}} \varphi \cdot Dv \right\}$$

- ▶ The Euler-Lagrange equations imply that the optimal φ is divergence free
- ▶ If the minimal v is binary, the calibration argument can be applied
- ▶ Can be solved via the PDHG algorithm [P., Cremers, Bischof, Chambolle, '09]
- ▶ Difficulty: Projection onto the convex set \mathcal{K}

Example

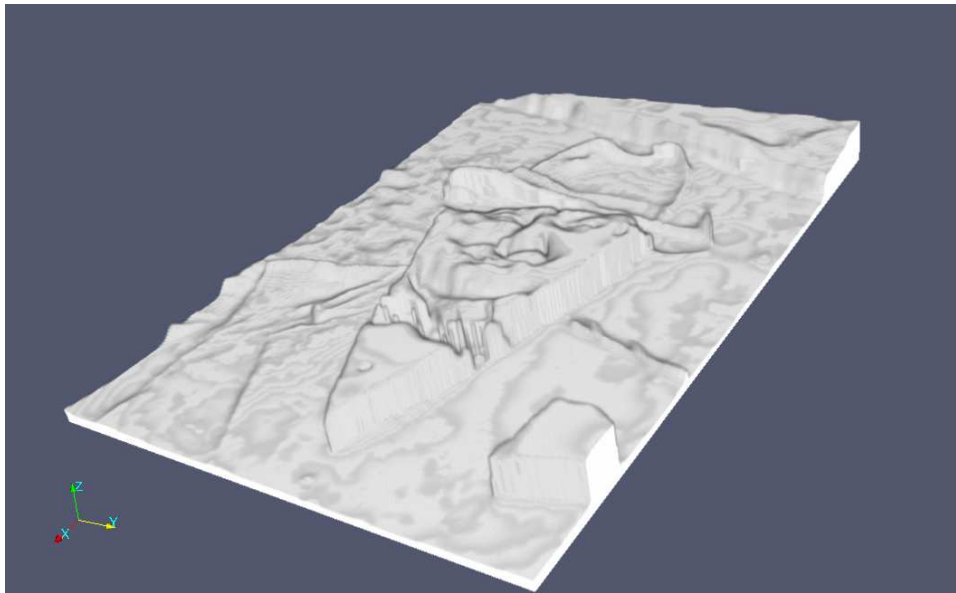


(a) original image f



(b) piecewise smooth image u

Visualization of the subgraph



(a) relaxed function v

The crack tip problem

Optimality shown in [Bonnet, David '01]

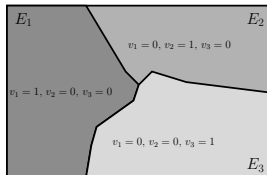


Phase-field approximation

Convex relaxation

Minimal partitions

- ▶ The “continuous” Potts model,
- ▶ Minimizes area of total interface subject to some given external fields f_i
- ▶ NP-hard for $k > 2$



- ▶ Convex relaxation

$$\min_{\mathbf{v}} \mathcal{J}_{1,2}(\mathbf{v}) + \sum_{i=1}^k \int_{\Omega} v_i f_i \, dx, \quad \text{s.t.} \quad v_i(x) \geq 0, \quad \sum_{i=1}^k v_i(x) = 1, \quad \forall x \in \Omega$$

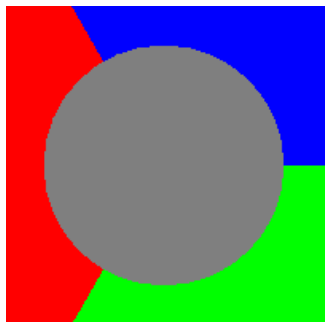
$$\mathcal{J}_1(\mathbf{v}) = \frac{1}{2} \sum_{i=1}^k \int_{\Omega} |Dv_i|, \quad [\text{Zach et al. '08}]$$

$$\mathcal{J}_2(\mathbf{v}) = \sup_{\mathbf{q} \in \mathcal{Q}} \int_{\Omega} \langle D\mathbf{v}, \mathbf{q} \rangle, \quad \mathcal{Q} = \left\{ \mathbf{q} \mid \|q_i - q_j\|_{2,\infty} \leq 1 \right\}, \quad [\text{Chambolle, Cremers, Pock, '11}]$$

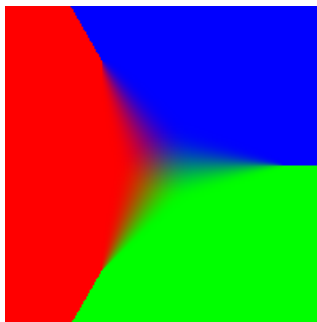
tv-potts.ipynb

The triple-junction problem in 2D

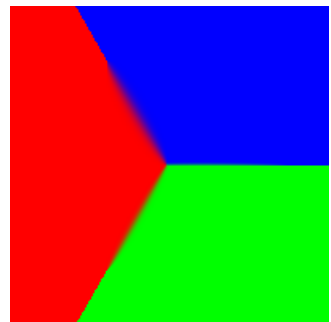
A comparison using the “triple-junction” problem



(a) Input



(b) \mathcal{J}_1



(c) \mathcal{J}_2

Image segmentation

Piecewise constant Mumford-Shah segmentation with $k = 16$ labels and using $f_i = (I - \mu_i)^2$



(a) Input



(b) Segmentation

Interactive image segmentation

Fitting gaussian mixture models to the user specified regions and iteratively updating the mixture models



(a) input image with user input



(b) segmentation

Phases



(a) phase 1



(b) phase 2

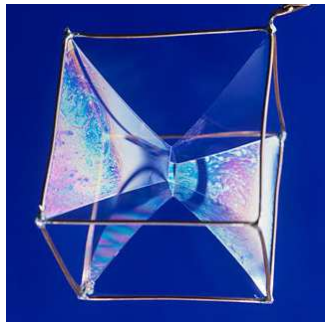


(c) phase 3



(d) phase 4

Minimal surfaces in 3D



(a) Soapfilm

(b) Minimal surface

Global solutions of non-convex models

- ▶ Consider the following non-convex energy-functional [P., Cremers, Bischof, Chambolle '10]

$$\min_u \int_{\Omega} f(x, u(x), \nabla u(x)) \, dx$$

- ▶ Can be solved via the calibration method as long as $f(x, u(x), \nabla u(x))$ is convex in ∇u

$$\min_{v \in BV(\Omega \times \mathbb{R}, [0,1])} \left\{ \sup_{\varphi \in \mathcal{K}} \int_{\Omega \times \mathbb{R}} \varphi \cdot Dv \right\},$$

where the convex set \mathcal{K} is given by

$$\mathcal{K} = \left\{ \varphi = (\varphi^x, \varphi^t) \mid \varphi^t(x, t) \geq f^*(x, t, \varphi^x(x, t)) \right\}$$

- ▶ Different convex regularizers: TV, Huber, Quadratic, Lipschitz, ...

Application to stereo



Input

Application to stereo



Data term only

Application to stereo



Convex variational approach

Application to stereo

Overview

Total Variation

Total generalized variation

Optical flow estimation

3D reconstruction

The Mumford-Shah functional

Total roto-translational variation

Subjective boundaries



- ▶ Human tend to “see” invisible boundaries that yield plausible objects.
- ▶ Important mechanism of the human visual system to interpret the 3D world under normal conditions.
- ▶ Provides strong clues for depth recognition [Nitzberg, Mumford, Shiota '93].
- ▶ Psychophysical experiments suggest that those boundaries are well modeled by **elastic curves** [Kanizsa '79].

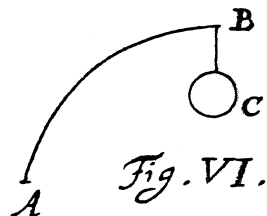
Subjective boundaries



- ▶ Human tend to “see” invisible boundaries that yield plausible objects.
- ▶ Important mechanism of the human visual system to interpret the 3D world under normal conditions.
- ▶ Provides strong clues for depth recognition [Nitzberg, Mumford, Shiota '93].
- ▶ Psychophysical experiments suggest that those boundaries are well modeled by **elastic curves** [Kanizsa '79].

The Elastica functional

- ▶ ...obtained from minimizers of the Elastica energy



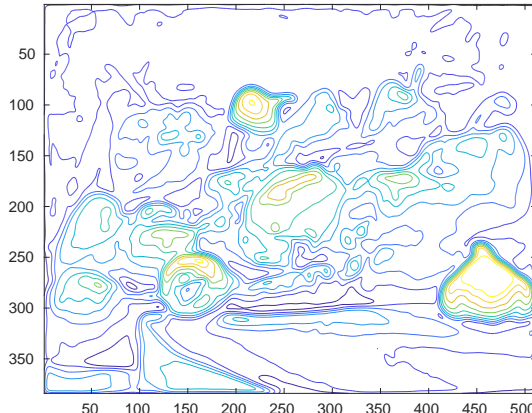
$$\int_{\Gamma} (1 + \alpha^2 |\kappa|^2) \, d\gamma, \quad \alpha > 0.$$

- ▶ Long history, dating back at least to Bernoulli (1691) and Euler (1744)

Generalization to images

The Elastic curve energy can be generalized to whole images by imposing the Elastica energy to each level line of an image $u \in \mathcal{C}_c^2(\Omega, \mathbb{R})$ [Masnou, Morel '98], [Ambrosio, Masnou '03]

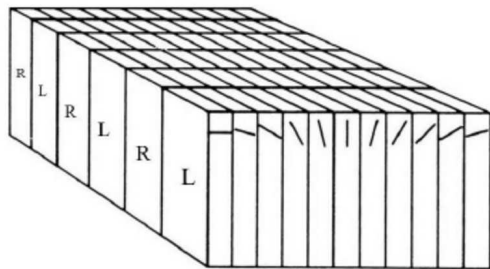
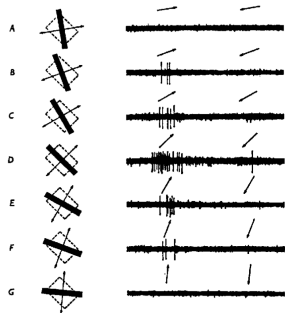
$$\int_{\Omega} \left(1 + \alpha^2 \left| \operatorname{div} \frac{\nabla u}{|\nabla u|} \right|^2 \right) d|\nabla u|,$$



Minimizing the Elastica energy

- ▶ The Elastica energy is highly non-convex and hence is difficult to minimize directly
- ▶ Involves higher-order derivatives and hence is difficult to discretize and minimize [Chan, Kang, Shen '03].
- ▶ Recent approaches are based on Augmented Lagrangian approaches, which amounts to solving a non-convex saddle-point problem [Tai, Hahn, Chung '11], [Yashtini, Kang '15], [Bae, Tai, Zhu '17], [Dweng, Glowinsky, Tai '18].
- ▶ Related methods exist in the PDE community, e.g. Weickert's EED [Weickert '96] or joint interpolation of vector fields and intensities [Ballester, Bertalmio, Caselles, Sapiro, Verdera '03]
- ▶ In shape processing, phase-field methods have successfully been used to minimize the Willmore energy [Franken, Rumpf, Wirth '10], [Dondl, Mugnai, Röger '13], [Bretin, Masnou, Oudet '13]

Visual cortex



- ▶ Experiments suggest that the visual cortex is made of orientation sensitive layers [Hubel, Wiesel '59]
- ▶ Cells are connected between the layers to get a sense of curvature at objects boundaries

Parametrized curves in the plane

- ▶ Consider the boundary of a smooth 2D set $E \subset \Omega \subseteq \mathbb{R}^2$ represented by a parametrized curve $\gamma(t) = (x_1(t), x_2(t))$ with parameter $t \in [0, 1]$.

Parametrized curves in the plane

- ▶ Consider the boundary of a smooth 2D set $E \subset \Omega \subseteq \mathbb{R}^2$ represented by a parametrized curve $\gamma(t) = (x_1(t), x_2(t))$ with parameter $t \in [0, 1]$.
- ▶ Its arc length variation is given by

$$\frac{ds}{dt} = |\dot{\gamma}(t)| = \sqrt{(\dot{x}_1(t))^2 + (\dot{x}_2(t))^2}$$

Parametrized curves in the plane

- ▶ Consider the boundary of a smooth 2D set $E \subset \Omega \subseteq \mathbb{R}^2$ represented by a parametrized curve $\gamma(t) = (x_1(t), x_2(t))$ with parameter $t \in [0, 1]$.
- ▶ Its arc length variation is given by

$$\frac{ds}{dt} = |\dot{\gamma}(t)| = \sqrt{(\dot{x}_1(t))^2 + (\dot{x}_2(t))^2}$$

- ▶ The tangential angle $\theta(t)$ is such that

$$\frac{\dot{\gamma}(t)}{|\dot{\gamma}(t)|} = (\cos \theta(t), \sin \theta(t))$$

Parametrized curves in the plane

- ▶ Consider the boundary of a smooth 2D set $E \subset \Omega \subseteq \mathbb{R}^2$ represented by a parametrized curve $\gamma(t) = (x_1(t), x_2(t))$ with parameter $t \in [0, 1]$.
- ▶ Its arc length variation is given by

$$\frac{ds}{dt} = |\dot{\gamma}(t)| = \sqrt{(\dot{x}_1(t))^2 + (\dot{x}_2(t))^2}$$

- ▶ The tangential angle $\theta(t)$ is such that

$$\frac{\dot{\gamma}(t)}{|\dot{\gamma}(t)|} = (\cos \theta(t), \sin \theta(t))$$

- ▶ The curvature κ_E of ∂E is defined as the ratio between the variation of the tangential angle θ and the variation of its length s , that is

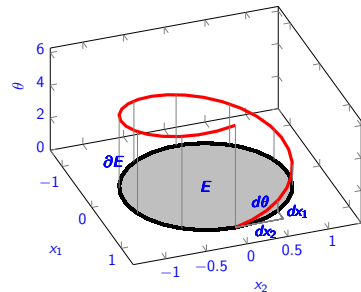
$$\kappa_E = \frac{d\theta}{ds} = \frac{\frac{d\theta}{dt}}{\frac{ds}{dt}} = \frac{\frac{d\theta}{dt}}{\sqrt{(\dot{x}_1(t))^2 + (\dot{x}_2(t))^2}}$$

Lifting the curve

- We now “lift” the 2D curve $\gamma(t)$ to a 3D curve $\Gamma(t) = (x_1(t), x_2(t), \theta(t))$ in the RT space $\Omega \times \mathbb{S}^1$:
- The length of the lifted curve is given by

$$\begin{aligned}\int_0^1 |\dot{\Gamma}(t)| dt &= \int_0^1 \sqrt{(\dot{x}_1(t))^2 + (\dot{x}_2(t))^2 + (\dot{\theta}(t))^2} dt \\ &= \int_0^1 \sqrt{1 + \frac{(\dot{\theta}(t))^2}{(\dot{x}_1(t))^2 + (\dot{x}_2(t))^2}} \sqrt{(\dot{x}_1(t))^2 + (\dot{x}_2(t))^2} dt \\ &= \int_0^L \sqrt{1 + \kappa_E^2} ds\end{aligned}$$

- Length of the curve in the lifted space has a “sense” of curvature!
- How can we generalize this to more general energies involving the curvature?



Normalized tangential field

- We define the tangential vector $p(t) = (p^x(t), p^\theta(t))$ where

$$p^x(t) = (\dot{x}_1(t), \dot{x}_2(t)), \quad p^\theta(t) = \dot{\theta}(t), \quad |p^x(t)| = \sqrt{(\dot{x}_1(t))^2 + (\dot{x}_2(t))^2}$$

- We further define the normalized tangential field $\tau(x, \theta) = (\tau^x(x, \theta), \tau^\theta(x, \theta))$ in $\Omega \times \mathbb{S}^1$

$$\tau(x(t), \theta(t)) = \frac{p(t)}{|p(t)|}, \quad \forall t \in [0, 1]$$

- The curvature is therefore given by

$$\kappa_E(t) = \frac{p^\theta(t)}{|p^x(t)|} = \frac{\tau^\theta(x(t), \theta(t))}{|\tau^x(x(t), \theta(t))|},$$

Curvature penalizing energies

- We consider $f : \mathbb{R} \rightarrow [0, +\infty]$ a convex, lower-semicontinuous function and want to define a lower-semicontinuous extension to energies of the type

$$E \mapsto \int_{\partial E} f(\kappa_E) \, d\mathcal{H}^1,$$

where $E \subset \Omega$ is a set with C^2 boundary, and κ_E is the curvature of the set.

- Using the normalized tangential vector field $\tau(x, \theta)$, the energy can be extended to $\Omega \times \mathbb{S}^1$:

$$\int_{\partial E} f(\kappa_E) \, d\mathcal{H}^1 = \int_{\Omega \times \mathbb{S}^1} f(\tau^\theta / |\tau^x|) |\tau^x| \, d\mathcal{H}^1 \llcorner \Gamma_E,$$

where Γ_E is the lifted curve.

- Note that the expression $f(\tau^\theta / |\tau^x|) |\tau^x|$ is in the form of the perspective of a convex function.

Different convex energies

$$\int_{\Omega \times \mathbb{S}^1} \textcolor{red}{f}(\tau^\theta / |\tau^x|) |\tau^x| \, d\mathcal{H}^1 \llcorner \Gamma_E$$

¹Also known as Reeds-Shepp model for cars [Reeds, Shepp '90]

Different convex energies

$$\int_{\Omega \times \mathbb{S}^1} \textcolor{red}{f}(\tau^\theta / |\tau^x|) |\tau^x| \, d\mathcal{H}^1 \llcorner \Gamma_E$$

- $f_1(s) = 1 + \alpha|s|$: Total Absolute Curvature

$$\int_{\Omega \times \mathbb{S}^1} |\tau^x| + \alpha |\tau^\theta| \, d\mathcal{H}^1 \llcorner \Gamma_E.$$

¹Also known as Reeds-Shepp model for cars [Reeds, Shepp '90]

Different convex energies

$$\int_{\Omega \times \mathbb{S}^1} f(\tau^\theta / |\tau^x|) |\tau^x| \, d\mathcal{H}^1 \llcorner \Gamma_E$$

- $f_1(s) = 1 + \alpha|s|$: Total Absolute Curvature

$$\int_{\Omega \times \mathbb{S}^1} |\tau^x| + \alpha |\tau^\theta| \, d\mathcal{H}^1 \llcorner \Gamma_E.$$

- $f_2(s) = \sqrt{1 + \alpha^2 |s|^2}$: Total Roto-Translational Variation ¹

$$\int_{\Omega \times \mathbb{S}^1} \sqrt{|\tau^x|^2 + \alpha^2 |\tau^\theta|^2} \, d\mathcal{H}^1 \llcorner \Gamma_E$$

¹Also known as Reeds-Shepp model for cars [Reeds, Shepp '90]

Different convex energies

$$\int_{\Omega \times \mathbb{S}^1} f(\tau^\theta / |\tau^x|) |\tau^x| \, d\mathcal{H}^1 \llcorner \Gamma_E$$

- $f_1(s) = 1 + \alpha|s|$: Total Absolute Curvature

$$\int_{\Omega \times \mathbb{S}^1} |\tau^x| + \alpha |\tau^\theta| \, d\mathcal{H}^1 \llcorner \Gamma_E.$$

- $f_2(s) = \sqrt{1 + \alpha^2 |s|^2}$: Total Roto-Translational Variation ¹

$$\int_{\Omega \times \mathbb{S}^1} \sqrt{|\tau^x|^2 + \alpha^2 |\tau^\theta|^2} \, d\mathcal{H}^1 \llcorner \Gamma_E$$

- $f_3(s) = 1 + \alpha^2 |s|^2$: Total Squared Curvature

$$\int_{\Omega \times \mathbb{S}^1} |\tau^x| + \alpha^2 \frac{|\tau^\theta|^2}{|\tau^x|} \, d\mathcal{H}^1 \llcorner \Gamma_E.$$

¹Also known as Reeds-Shepp model for cars [Reeds, Shepp '90]

Different convex energies

$$\int_{\Omega \times \mathbb{S}^1} f(\tau^\theta / |\tau^x|) |\tau^x| \, d\mathcal{H}^1 \llcorner \Gamma_E$$

- $f_1(s) = 1 + \alpha|s|$: Total Absolute Curvature

$$\int_{\Omega \times \mathbb{S}^1} |\tau^x| + \alpha |\tau^\theta| \, d\mathcal{H}^1 \llcorner \Gamma_E.$$

- $f_2(s) = \sqrt{1 + \alpha^2 |s|^2}$: Total Roto-Translational Variation ¹

$$\int_{\Omega \times \mathbb{S}^1} \sqrt{|\tau^x|^2 + \alpha^2 |\tau^\theta|^2} \, d\mathcal{H}^1 \llcorner \Gamma_E$$

- $f_3(s) = 1 + \alpha^2 |s|^2$: Total Squared Curvature

$$\int_{\Omega \times \mathbb{S}^1} |\tau^x| + \alpha^2 \frac{|\tau^\theta|^2}{|\tau^x|} \, d\mathcal{H}^1 \llcorner \Gamma_E.$$

Convex energies in the measure $\sigma = \tau \, d\mathcal{H}^1 \llcorner \Gamma_E$

¹Also known as Reeds-Shepp model for cars [Reeds, Shepp '90]

The measure σ

The measure $\sigma = \tau \, d\mathcal{H}^1 \llcorner \Gamma_E$ is not arbitrary: It satisfies two important constraints:

- (i) By construction, it is a circulation and has zero divergence in $\Omega \times \mathbb{S}^1$ since we want to represent closed curves (or ending at the boundary).
- (ii) Its marginals in $\Omega \times \mathbb{S}^1$, denoted by $\bar{\sigma} = \int_{\mathbb{S}^1} \sigma^x$ also have zero divergence.
- (iii) It follows that there exists a BV function u such that $Du^\perp = \bar{\sigma}$, here u is the characteristic function of the set E .

Convex representation

- We define the following convex function

$$h(\theta, p) = \begin{cases} |p^x|f(p^\theta / |p^x|) & \text{if } p^x \in \mathbb{R}_+ \theta, p^x \neq 0, \\ f^\infty(p^\theta) & \text{if } p^x = 0, \\ +\infty & \text{else.} \end{cases},$$

where $f^\infty(t) = \lim_{s \rightarrow 0} sf(t/s)$ is the recession function of f .

- This function encodes the sub-Riemannian structure of $\Omega \times \mathbb{S}^1$.
- It is well known that h is a one-homogeneous function, hence the support function of a convex set, that is

$$h(\theta, p) = \sup_{\xi \in H(\theta)} \xi \cdot p$$

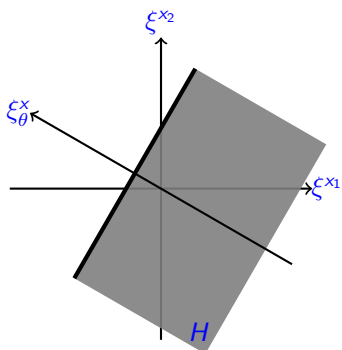
where the convex set $H(\theta)$ is given by:

$$H(\theta) = \{\xi = (\xi^x, \xi^\theta) \in \mathbb{R}^3 : \xi^x \cdot \underline{\theta} \leq -f^*(\xi^\theta)\}, \quad \underline{\theta} = (\cos \theta, \sin \theta)$$

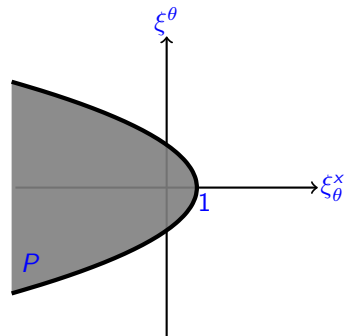
Visualization of the set $H(\theta)$

Example using $f(t) = 1 + \alpha^2 t^2$ (Elastica):

$$H(\theta) = \{\xi = (\xi^x, \xi^\theta) \in \mathbb{R}^3 : \xi^x \cdot \underline{\theta} + \frac{(\xi^\theta)^2}{(2\alpha)^2} \leq 1\}$$



(a) $H \cap \{(\xi^x, \xi^\theta) : \xi^x \in \mathbb{R}^2, \xi^\theta = 0\}$



(b) Profile P

The functional

- We introduce the following functional:

$$F(u) = \inf \left\{ \int_{\Omega \times \mathbb{S}^1} h(\theta, \sigma) : \operatorname{div} \sigma = 0, \bar{\sigma} = Du^\perp \right\}$$

- In general, σ is a bounded Radon measure, therefore the correct way to write the energy is rather

$$\int_{\Omega \times \mathbb{S}^1} h\left(\theta, \frac{\sigma}{|\sigma|}\right) d|\sigma|.$$

and the constraints are understood in the weak sense.

- We assume that $f(t) \geq \gamma \sqrt{1+t^2}$ such that

$$F(u) \geq \gamma \int_{\Omega \times \mathbb{S}^1} |\sigma| \geq \gamma \int_{\Omega} |Du|$$

- It can be shown that the functional is convex, lower-semicontinuous on $BV(\Omega)$, since

$$\int_{\Omega \times \mathbb{S}^1} h(\theta, \sigma) = \sup_{\varphi(x, \theta) \in H(\theta)} \int_{\Omega \times \mathbb{S}^1} \varphi \cdot \sigma$$

Tightness of the representation

We can show the following result:

Theorem

Let $E \subset \Omega$ be a set with C^2 boundary. Then

$$F(\chi_E) = \int_{\partial E \cap \Omega} f(\kappa_E(x)) d\mathcal{H}^1(x).$$

- ▶ The proof is based on Smirnov's theorem (1994), which shows that if σ is a measure with $\operatorname{div} \sigma = 0$ then it is a superposition of curves.
- ▶ We conjecture that our result can be extended to general BV functions u with C^2 level sets, hence coinciding with Masnou and Morel's model.
- ▶ We could hope that $F(u)$ is the lower-semicontinuous envelope of the original functional, however, simple examples show that this is not the case [Bellettini, Mugnai '04/'05], [Dayrens, Masnou '16].

Dual representation

- ▶ Recall our primal functional

$$F(u) = \inf \left\{ \int_{\Omega \times \mathbb{S}^1} h(\theta, \sigma) : \operatorname{div} \sigma = 0, \bar{\sigma} D u^\perp \right\}.$$

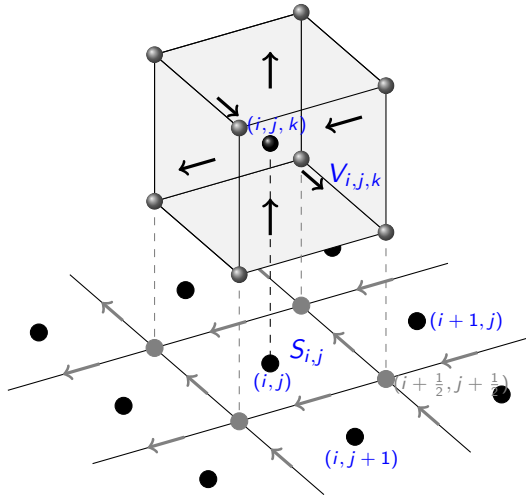
- ▶ It has the following dual representation

$$\begin{aligned} F(u) &= \sup \left\{ \int_{\Omega} \psi \cdot D u^\perp : \psi \in C_c^0(\Omega; \mathbb{R}^2), \right. \\ &\quad \left. \exists \varphi \in C_c^1(\Omega \times \mathbb{S}^1), \underline{\theta} \cdot (\nabla_x \varphi + \psi) + f^*(\partial_\theta \varphi) \leq 0 \right\}. \end{aligned}$$

- ▶ Coincides with the dual representation in our previous work [Bredies, P. Wirth '15] which is based on an explicit lifting of the curvature variable.
- ▶ In our approach the curvature variable appears naturally as the derivative of the orientation.

Discretization

- ▶ We use a staggered 2D-3D averaged Raviart-Thomas finite elements discretization based on cubes.
- ▶ Divergence-conforming discretization, uses a cube-center-based quadrature rule for the energy.
- ▶ We can show consistency of the discretization up to small oscillations.



Discrete Problem

- We consider discrete optimization problems of the form

$$\min_u F_\delta(u) + G_\delta(u),$$

with

$$F_\delta(u) = \min_{\sigma} \left\{ \delta_x^2 \delta_\theta \sum_{\mathbf{j}=(i,j,k) \in \mathcal{J}} h(k\delta_\theta, (\mathcal{A}\sigma)_{\mathbf{j}}) : \mathcal{D}\sigma = 0, \mathcal{P}\sigma - \mathcal{G}u = 0 \right\}.$$

- We solve this non-smooth convex optimization problem by considering its Lagrangian

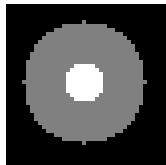
$$\begin{aligned} \min_{u, \sigma} \max_{\phi, \psi, \xi} & \sum_{\mathbf{j} \in \mathcal{J}} (\mathcal{A}\sigma)_{\mathbf{j}} \cdot \xi_{\mathbf{j}} - \sum_{\mathbf{j}=(i,j,k) \in \mathcal{J}} h^*(k\delta_\theta, \xi_{\mathbf{j}}) + G_\delta(u) + \\ & \sum_{\mathbf{j} \in \mathcal{J}} (\mathcal{D}\sigma)_{\mathbf{j}} \phi_{\mathbf{j}} + \sum_{\mathbf{i} \in \mathcal{I}^1 \cup \mathcal{I}^2} ((\mathcal{P}\sigma)_{\mathbf{i}} - (\mathcal{G}u)_{\mathbf{i}}) \psi_{\mathbf{i}}, \end{aligned}$$

- We solve the saddle-point problem with a pre-conditioned first-order primal-dual algorithm.

First experiment: computing a disk

- ▶ Consider the Elastica energy for the boundary of a disk

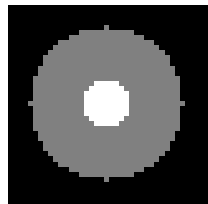
$$\int_{\partial B(0,r)} (1 + \alpha^2 \kappa^2) d\mathcal{H}^1 = 2\pi(r + \alpha^2/r)$$



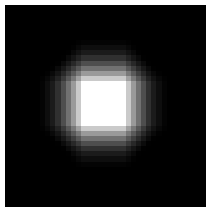
- ▶ The energy is minimized for $r = 1/\alpha$.
- ▶ We study the effect of different discretizations of the angular dimension by computing (via inpainting) a disk of radius $r = 10$.

N_θ	H_{TV} ($2\pi r \approx 62.83$)	H_{AC} ($2\pi \approx 6.28$)	H_{SC} ($2\pi/r \approx 0.62$)
4	60.10	6.34	1.75
8	54.80	6.28	0.89
16	58.50	6.28	0.70
32	61.52	6.28	0.64
64	62.93	6.28	0.62

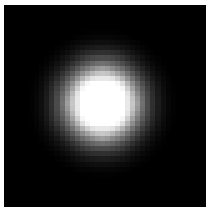
Disk inpainting



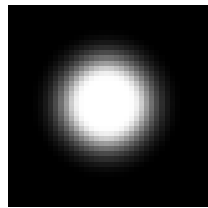
(a) u^0



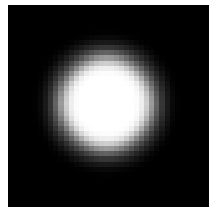
(b) $N_\theta = 4$



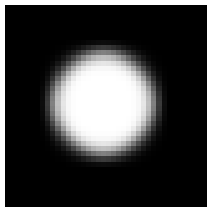
(c) $N_\theta = 8$



(d) $N_\theta = 16$

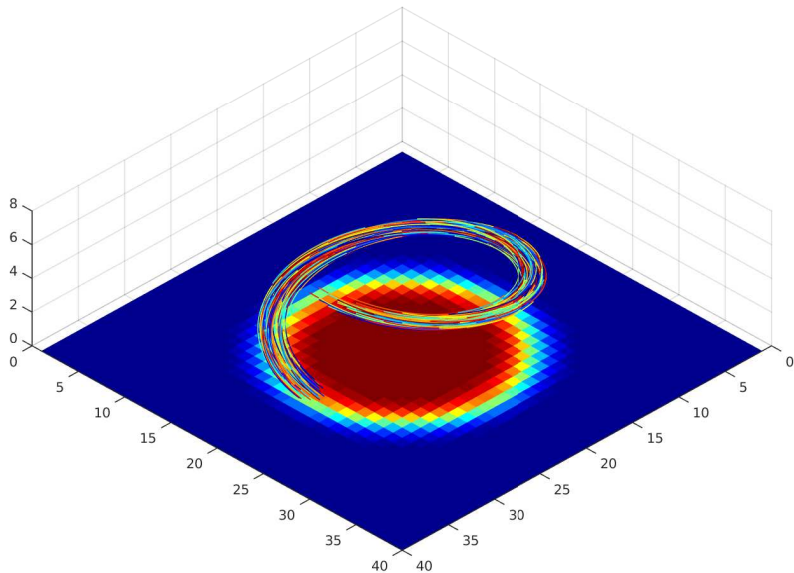


(e) $N_\theta = 32$



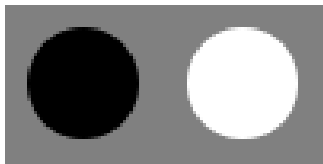
(f) $N_\theta = 64$

Visualization of the measure σ



Where it fails: Non-smooth level sets

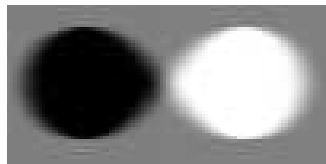
- We consider the following inpainting problem by minimizing the Elastica energy.



(a) Original image



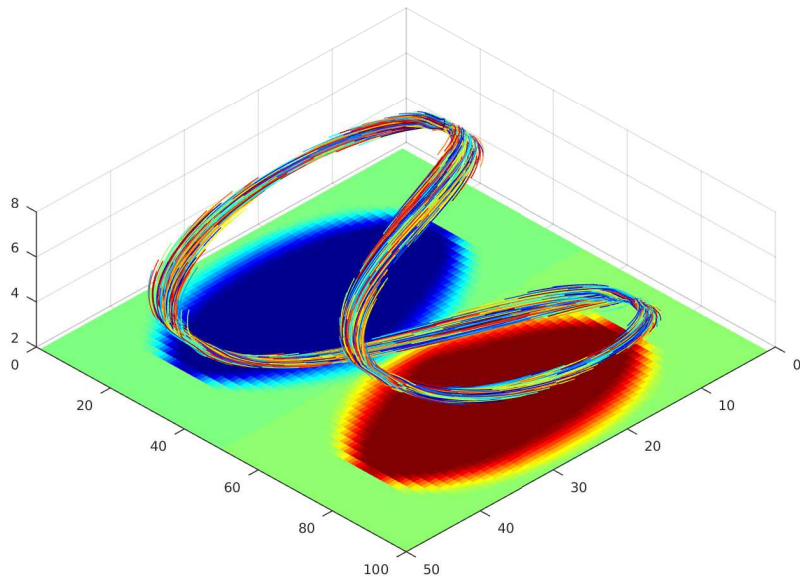
(b) Input image u^0



(c) Computed image u

- The energy of the original Elastica energy should be infinite
- Our convexification finds a lower energy solutions with non-smooth level sets

Visualization of the measure σ



Shape regularization

- We consider the problem of regularizing a given shape



Shape regularization



(a) TAC, $\lambda = 8$

(b) TAC, $\lambda = 4$

(c) TAC, $\lambda = 2$

Shape regularization



(a) TRV, $\lambda = 8$

(b) TRV, $\lambda = 4$

(c) TRV, $\lambda = 2$

Shape regularization



(a) TSC, $\lambda = 8$



(b) TSC, $\lambda = 4$

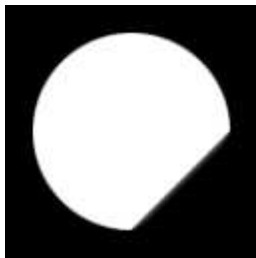


(c) TSC, $\lambda = 2$

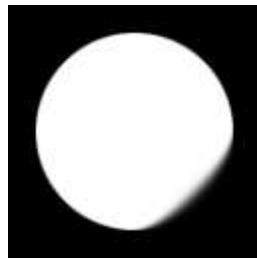
Shape completion (1)



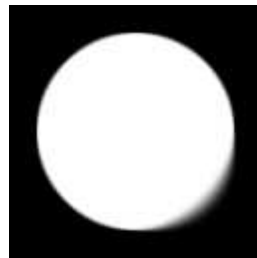
(a) Input image



(b) TAC, $\alpha = 15$



(c) TRV, $\alpha = 15$



(d) TSC, $\alpha = 50$



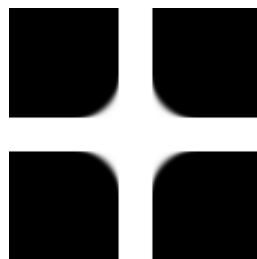
(e) Input image



(f) TAC, $\alpha = 15$



(g) TRV, $\alpha = 15$



(h) TSC, $\alpha = 10$

Shape completion (2)



(a) Input image



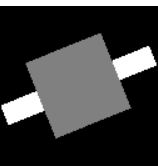
(b) TAC, $\alpha = 15$



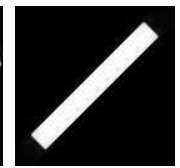
(c) TRV, $\alpha = 15$



(d) TSC, $\alpha = 10$



(e) Input images with rotations $0, \pi/8, \pi/4$



(f) TAC, $\alpha = 15$

Weickert's cat

- ▶ Shape reconstruction from “dipole” data
- ▶ The dipoles are original data from J. Weickert.



Dipole data

Weickert's cat

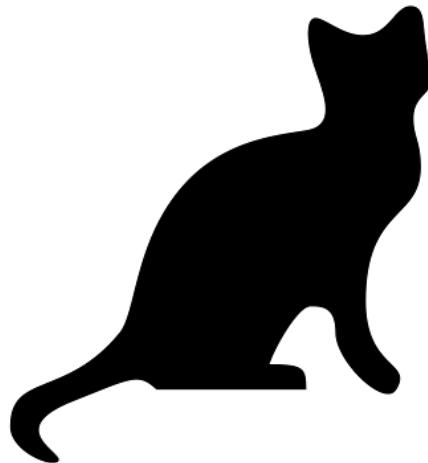
- ▶ Shape reconstruction from “dipole” data
- ▶ The dipoles are original data from J. Weickert.



Minimizing the TSC energy

Weickert's cat

- ▶ Shape reconstruction from “dipole” data
- ▶ The dipoles are original data from J. Weickert.



Original shape

Image inpainting



Input

Image inpainting



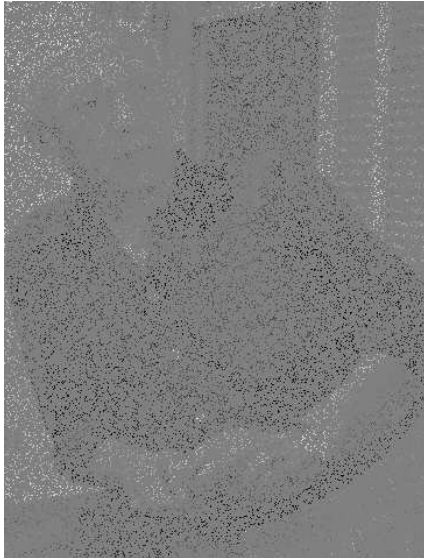
TV

Image inpainting



TSC

Image inpainting



Input

Image inpainting



TV

Image inpainting



TSC

Image denosing: Guassian noise



Input

Image denosing: Guassian noise



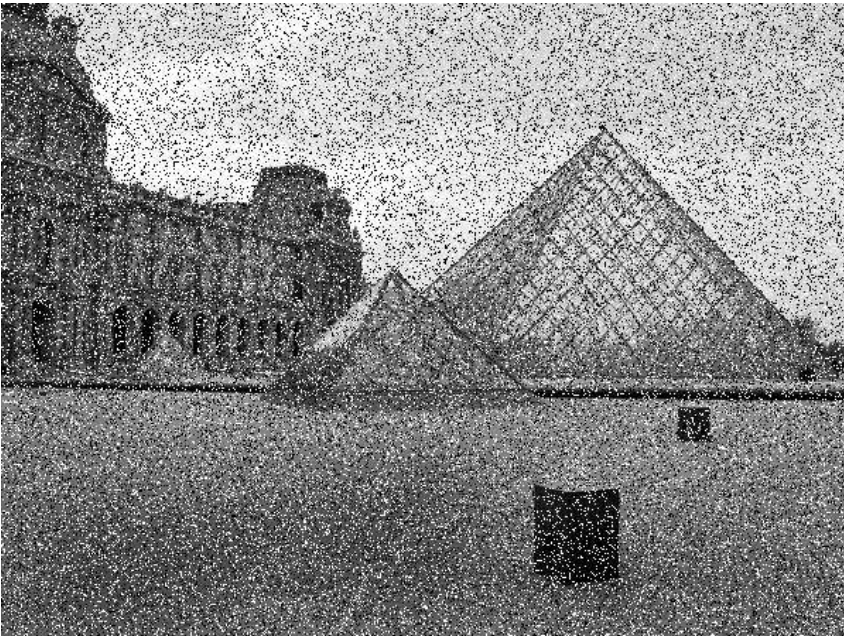
TV, $\alpha = 0, \lambda = 10$

Image denosing: Guassian noise



TSC, $\alpha = 10$, $\lambda = 40$

Image denosing: S & P noise



Input

Image denosing: S & P noise



TV, $\alpha = 0, \lambda = 2$

Image denosing: S & P noise



TSC, $\alpha = 10$, $\lambda = 7$